Supporting Information

Two luminescent film sensors constructed by new lanthanide coordination polymers for ratiometric detection of Zn^{2+} and NH_3 in water and their white emission properties

Hui Wang, [a] *Xuan Li,* [a] *Hao Cheng,* [a]*Ya-Jun Li,*[a]*Xue-Qin Song*,* [a] *Li, Wang**[b,c]

a. School of Chemistry and Chemical Engineering, Lanzhou Jiaotong University, Lanzhou, 730070, China.
b. College of Chemistry and Chemical Engineering, Xi'an Shiyou University, Xi'an, 710065, China.
c. State Key Laboratory of Coordination Chemistry, School of Chemistry and Chemical Engineering, Nanjing University, Nanjing, 210093, China.

Contents

Materials and methods

Anhydrous pyridine was treated with CaH_2 and distilled. Other solvents and chemicals were from commercial sources without further purification. $Tb(NO_3)_3 \cdot 6H_2O$ was prepared by dissolving oxides Tb_4O_7 in concentrated nitric acid and hydrogen peroxide followed by evaporation and crystallization. $Eu(NO_3)_3 \cdot 6H_2O$ were prepared with the same method without using hydrogen peroxide.

^{1}H NMR spectra of **L** was recorded in $CDCl_3$ solution at room temperature on a Bruker 500 instrument and referenced to tetramethylsilane (0.00 ppm) as an internal standard. Infrared spectra (4000~400 cm^{-1}) were obtained on a Therrno Mattson FTIR spectrometer. Thermogravimetric analysis experiments were performed using a TGA/NETZSCH STA449C instrument heated from 30~800°C (heating rate of 10 °C/min, N_2 stream). X-ray powder diffraction (XRPD) patterns of samples were recorded on a X-ray diffractometer (Rigaku D/Max 2200PC) in the 2θ range from 5° to 50° at room temperature. Simulation of the PXRD pattern was carried out with the single-crystal X-ray diffraction data using Mercury software (version: 3.10). The high-resolution scanning electron microscopy (HRSEM) images were taken on a JSM-6701F Cold-field emission scanning electron microscope. Solid UV-Vis spectra were recorded with Cary Series UV-Vis-NIR Spectrophotometer. The phosphorescence spectrum was used phosphorescence spectrophotometer to record. Luminescence excitation and emission spectra in visible range were obtained at F-7000 fluorescence spectrophotometer (Japan Hitachi company) at room temperature with samples putting between quartz plates. Luminescence lifetime measurements were determined by a single-photon counting spectrometer using an Edinburgh FLS920 spectrometer equipped with a continuous Xe900 xenon lamp with the corrections of excitation and emission for the detector response performed from 200 to 900 nm. The theoretical calculation for compounds were performed with the GAUSSIAN09 program at the B3LYP/Gen level (the 6-31 G basis set for C, H, O and N, and the LANL2DZ basis set for the metal atoms) to model the initial guess of the title compounds obtained from the X-ray refinement data (CIF). The SEM photograph of EuL/TbL@PMMA was recorded with JSM-6700F field emission scanning electron microscope. Spin-coated films and doped film are prepared by Laurell WS-650Mz-23NPPB. The tensile test of the film is recorded by the large deformation electronic universal testing machine WDW-10M.

X-ray Crystallographic Study

Diffraction data on single crystals of **EuL**, **TbL** and **GdL** were recorded with a Bruker Smart Apex II CCD diffractometer using the ω-scan mode. No crystal decay was observed during the data collections. The three structures were solved by direct methods and refined on F^2 by a full-matrix least-squares procedure. SHELXL-2014 was used for both structure solutions and refinements.[1] Crystallographic diagrams were drawn using the DIAMOND software package.[2] A summary of the relevant crystallographic data and the final refinement details are given in Table S1, important bond lengths and angles are listed in Table S2.

Detection of Zn^{2+}, NH_3 in water media using EuL/TbL@PMMA

The metal nitrate solution (1×10^{-2} M) used in the test was prepared with deionized water and preserved before use. Solutions of Zn^{2+} ions with different concentration gradients from 10^{-3} to 10^{-5} M were obtained by dilution of 1×10^{-2} M Zn^{2+} solution successively.[3] The testing films were obtained by cutting **EuL**/**TbL**@PMMA into 0.5 × 0.5 cm pieces. For the luminescence response for metal cations, the small cut films were immersed in 1×10^{-2} M metal nitrate solution (M^{n+} = K^+, Ca^{2+}, Na^+, Mg^{2+}, Al^{3+}, Zn^{2+}, Fe^{3+}, Co^{2+}, Ni^{2+}, Cu^{2+}, Ag^+, Pb^{2+}, Hg^{2+} and Cd^{2+}) for 15 minutes respectively. While for interference experiment, the small cut film samples were immersed in a mixed solution of one kind of metal ions and Zn^{2+} ions for 15 minutes. The emission spectra of all the immersed films were determined with exciting wavelength of 315 nm at the excitation slit of 2.5 nm and emission slit of 1.0 nm after taken out and dried in a vacuum for 12 hours. For sensing NH_3, the 0.5 × 0.5 cm **EuL**/**TbL**@PMMA films pieces were used for sensing experiments. Both of these were placed into a vial comprising about 2 mL of various solutions containing amines (diethylamine, ethylenediamine, dipropylamine, propylamine, triethylamine, tripropylamine, triethanolamine, benzylamine). After soak for 12 h, photographs of **EuL**/**TbL**@PMMA films pieces were taken, followed by measurements of their luminescence spectra.

Table S1 Crystal data and structure refinement parameters for **EuL**,**TbL** and **GdL**

CCDC No	1980285	1980286	2116401
Empirical formula	$C_{51}H_{46}N_7EuO_{15}$	$C_{51}H_{46}N_7TbO_{15}$	$C_{51}H_{46}N_7GdO_{15}$
Temperature (K)	273(2)	273(2)	273(2)
M	1148.92	1155.87	1154.20
Crystal system, Space group	Monoclinic, $P2_1$ / c	Monoclinic, $P2_1$ / c	Monoclinic, $P2_1$ / c
Unit cell dimensions	*a* =10.2028(2)Å;	*a* = 10.1840(2)Å;	*a* = 10.1478(4)Å;
	b=20.5606(4)Å;β =95.048(10)°	*b* = 20.5165(5)Å; β =95.052(10)°	*b=20.3871(9)*Å; β =95.103(2)°
	c = 27.5955(6)Å;	c = 27.5390(7) Å;	c = 27.1677(14)Å;
V/Å^3, Z	5766.9(2), 4	5731.7(2), 4	5592.3(4),4
D_{calcd}/Mg m^{-3}	1.323	1.339	1.369
μ/mm^{-1}	1.154	1.301	1.253
F(000)	2336.0	2344.0	2340.0
Θ range for data collection	2.82° ~ 28.28°	2.78° ~ 27.26°	2.249° ~25.726°
index ranges, *hkl*	-13≤ h ≤ 13	-13 ≤ h ≤ 13	-12≤ h ≤ 12
	-27≤ k ≤ 27	-26 ≤ k ≤ 26	-23≤ k ≤24
	-36≤ l ≤ 36	-35 ≤ l ≤ 35	-33≤ l ≤ 33
Independent reflections (R_{int})	0.0248	0.0524	0.0742
Completeness	100%	99.7%	100%
Reflections collected/unique	87199 / 14358	84512 / 13198	59283/10661
Data / restraints / params	14358 / 0 / 671	13198 / 0 / 667	10661/0/667
Goodness–of–fit on F^2	1.042	1.046	1.018
Final *R* indices [$I > 2\sigma(I)$]	R_1 = 0.0262, wR_2 = 0.0771	R_1 = 0.0352, wR_2 = 0.0806	R_1 =0.0284,wR_2 =0.0602
R indices (all data)	R_1 = 0.0332, wR_2 = 0.0812	R_1 = 0.0565, wR_2 = 0.0900	R_1 =0.0393, wR_2 =0.0646

Table S2 Continuous Shape Measures calculation of **EuL**,**TbL** and **GdL**

Ideal structures		CShM		
		EuL	**TbL**	**GdL**
EP-9	(Enneagon)	0.3020	0.3039	0.3044
OPY-9	(Octagonal pyramid)	0.2738	0.2741	0.2739
HBPY-9	(Heptagonal bipyramid)	0.2544	0.2555	0.2546
JTC-9	(Johnson triangular cupola J3)	0.2262	0.2264	0.2270
JCCU-9	(Capped cube J8)	0.1762	0.1754	0.1729
CCU-9	(Spherical-relaxed capped cube)	0.2197	0.2192	0.2166
JCSAPR-9	(Capped square antiprism J10)	0.1758	0.1752	0.1729
CSAPR-9	(Spherical capped square antiprism)	0.1979	0.1969	0.1945
JTCTPR-9	(Tricapped trigonal prism J51)	0.1775	0.1763	0.1733
TCTPR-9	(Spherical tricapped trigonal prism)	0.1971	0.1964	0.1946
JTDIC-9	(Tridiminished icosahedron J63)	0.2355	0.2354	0.2320
HH-9	(Hula-hoop)	0.2256	0.2247	0.2232
MFF-9	(Muffin)	0.1926	0.1915	0.1896

Table S3 Selected bond lengths (Å) and angles (˚) for **EuL**,**TbL** and **GdL**

$[EuL(NO_3)_3]_n \cdot 2C_4H_8O_2$ (**EuL**)							
Eu1−N1	2.5847(17)	Eu1−O4	2.3821(15)	Eu1−O6	2.3307(15)	Eu1−O7	2.4763(19)
Eu1−O8	2.4600(2)	Eu1−O10	2.4668(17)	Eu1−O11	2.4839(18)	Eu1−O13	2.4346(16)
Eu1−O14	2.5261(17)						
O4−Eu1−N1	80.43(6)	O4−Eu1−O7	148.29(7)	O4−Eu1−O8	148.36(6)		
O4−Eu1−O10	124.21(6)	O4−Eu1−O11	72.83(6)	O4−Eu1−O13	85.27(6)		
O4−Eu1−O14	78.79(5)	O6−Eu1−N1	86.26(6)	O6−Eu1−O4	84.56(5)		
O6−Eu1−O7	73.67(7)	O6−Eu1−O8	124.20(7)	O6−Eu1−O10	82.69(6)		
O6−Eu1−O11	75.76(7)	O6−Eu1−O13	150.80(6)	O6−Eu1−O14	151.04(6)		
O7−Eu1−N1	75.49(7)	O7−Eu1−O11	121.65(7)	O7−Eu1−O14	109.95(7)		
O8−Eu1−N1	88.01(8)	O8−Eu1−O7	51.26(8)	O8−Eu1−O10	76.89(7)		
O8−Eu1−O11	123.12(8)	O8−Eu1−O14	69.57(7)	O10−Eu1−N1	151.53(6)		
O10−Eu1−O7	76.24(7)	O10−Eu1−O11	51.39(6)	O10−Eu1−O14	126.27(6)		
O11−Eu1−N1	148.86(6)	O11−Eu1−O14	120.49(6)	O13−Eu1−N1	118.81(6)		
O13−Eu1−O7	124.47(8)	O13−Eu1−O8	74.67(7)	O13−Eu1−O10	80.61(6)		
O13−Eu1−O11	75.10(7)	O13−Eu1−O14	51.06(6)	O14−Eu1−N1	67.81(6)		
$[TbL(NO_3)_3]_n \cdot 2C_4H_8O_2$ (**TbL**)							
Tb1−N1	2.556(3)	Tb1−O2	2.303(2)	Tb1−O4	2.356(2)	Tb1−O7	2.432(3)
Tb1−O8	2.450(3)	Tb1−O10	2.507(2)	Tb1−O11	2.407(2)	Tb1−O13	2.440(2)
Tb1−O14	2.463(2)						
O2−Tb1−N1	86.19(8)	O2-Tb1-O4	84.26(8)	O2-Tb1-O7	124.83(9)		
O2−Tb1−O8	73.82(10)	O2-Tb1-O10	150.70(8)	O2-Tb1-O11	150.36(9)		
O2−Tb1−O13	83.10(9)	O2-Tb1-O14	75.64(9)	O4-Tb1-N1	80.45(8)		
O4−Tb1−O7	148.16(9)	O4-Tb1-O8	148.30(9)	O4-Tb1-O10	78.75(8)		
O4−Tb1−O11	85.24(8)	O4-Tb1-O13	124.72(8)	O4-Tb1-O14	72.89(8)		
O7−Tb1−N1	88.25(10)	O7-Tb1-O8	51.74(10)	O7-Tb1-O10	69.43(9)		
O7−Tb1−O13	76.27(10)	O7-Tb1-O14	122.85(10)	O8-Tb1-N1	75.59(9)		
O8−Tb1−O10	110.07(9)	O8-Tb1-O14	121.40(9)	O10-Tb1-N1	67.65(8)		
O11−Tb1−N1	119.18(8)	O11-Tb1-O7	74.46(10)	O11-Tb1-O8	124.62(10)		
O11−Tb1-O10	51.59(8)	O11-Tb1-O13	80.31(9)	O11-Tb1-O14	74.79(9)		
O13-Tb1-N1	151.14(9)	O13-Tb1-O8	75.71(9)	O13-Tb1-O10	126.20(8)		
O13-Tb1-O14	51.84(8)	O14-Tb1-N1	148.90(9)	O14-Tb1-O10	120.69(8)		
$[GdL(NO_3)_3]_n \cdot 2C_4H_8O_2$ (**GdL**)							
Gd1−N1	2.548(2)	Gd1−O2	2.3192(17)	Gd1−O6	2.3685(18)	Gd1−O7	2.4627(18)
Gd1−O8	2.4689(19)	Gd1−O10	2.4751(2)	Gd1−O11	2.4504(2)	Gd1−O13	2.5184(17)
Gd1−O14	2.4247(18)						
O2−Gd1−O4	83.17(6)	O2−Gd1−O7	82.68(6)	O2−Gd1−O8	75.55(7)		
O2−Gd1−O10	73.89(7)	O2−Gd1−O11	125.37(7)	O2−Gd1−O13	149.97(6)		
O2−Gd1−O14	150.71(7)	O2−Gd1−N1	85.65(7)	O2−Gd1−N5	76.05(7)		
O2−Gd1−N6	99.79(7)	O2−Gd1−N7	166.55(7)	O6−Gd1−O7	124.83(6)		
O6−Gd1−O8	72.71(6)	O6−Gd1−O10	147.23(6)	O6−Gd1−O11	148.09(6)		
O6−Gd1−O13	78.40(6)	O6−Gd1−O14	87.02(7)	O6−Gd1−N1	79.41(7)		
O6−Gd1−N	598.76(7)	O6−Gd1−N6	160.19(7)	O6−Gd1−N7	83.51(6)		
O7−Gd1−O8	52.13(6)	O7−Gd1−O10	75.64(6)	O7−Gd1−O13	127.35(6)		
O7−Gd1−N1	151.21(7)	O7−Gd1−N5	26.10(7)	O7−Gd1−N6	74.94(7)		
O7−Gd1−N7	103.56(6)	O8−Gd1−O10	121.75(6)	O8−Gd1−O13	120.11(6)		
O8−Gd1−N1	147.83(7)	O8−Gd1−N5	26.15(7)	O8−Gd1−N6	127.06(7)		
O8−Gd1−N7	98.67(7)	O10−Gd1−O13	110.93(6)	O10−Gd1−N1	75.86(7)		

Table S4 TD-DFT calculated electronic excitations of coordinated ligand **L**

state	Excitation(eV)	$\lambda_{excitation}$(nm)	Osc.strength (f)	Key transitions	Character	λ_{expt}
Singlet Excited States						
S_1	4.0314	307.55	0.0882	(16%) HOMO−15→LUMO	π→π*	332
				(22%) HOMO−7→LUMO	π→π*	
				(29%) HOMO−3→LUMO	π→π*	
				(55%) HOMO→LUMO	π→π*	
Triplet Excited States						
T_1	2.3953	517.61		(14%) HOMO−18→LUMO	π→π*	
				(13%) HOMO−3→LUMO	π→π*	
				(65%) HOMO→LUMO	π→π*	
				(10%) HOMO→LUMO	π→π*	
T_2	3.4202	362.51		(20%) HOMO−15→LUMO	π→π*	
				(35%) HOMO−7→LUMO	π→π*	
				(49%) HOMO−3→LUMO	π→π*	
				(15%) HOMO→LUMO	π→π*	
T_3	3.5579	348.48		(21%) HOMO−16→LUMO+3	π→π*	
				(12%) HOMO−12→LUMO+3	π→π*	
				(17%) HOMO−10→LUMO+3	π→π*	
				(15%) HOMO−9→LUMO+3	π→π*	
				(15%) HOMO−6→LUMO+3	π→π*	
				(11%) HOMO−5→LUMO+3	π→π*	
				(11%) HOMO−1→LUMO+2	π→π*	
				(39%) HOMO−1→LUMO+3	π→π*	
				(25%) HOMO−1→LUMO+3	π→π*	
T_4	3.5732	346.98		(16%) HOMO−17→LUMO+2	π→π*	
				(27%) HOMO−14→LUMO+2	π→π*	
				(11%) HOMO−9→LUMO+2	π→π*	
				(19%) HOMO−8→LUMO+2	π→π*	
				(20%) HOMO−5→LUMO+2	π→π*	
				(10%) HOMO−5→LUMO+9	π→π*	
				(15%) HOMO−5→LUMO+12	π→π*	
				(20%) HOMO−4→LUMO+2	π→π*	
				(10%) HOMO−4→LUMO-9	π→π*	
				(15%) HOMO−4→LUMO+12	π→π*	
				(27%) HOMO−2→LUMO+2	π→π*	
				(10%) HOMO−2→LUMO+2	π→π*	
T_5	3.6299	341.56		(32%) HOMO−15→LUMO	π→π*	
				(11%) HOMO−11→LUMO	π→π*	
				(10%) HOMO−10→LUMO	π→π*	
				(50%) HOMO−7→LUMO	π→π*	
				(25%) HOMO−3→LUMO	π→π*	
T_6	3.7859	327.49		(12%) HOMO−15→LUMO	π→π*	
				(23%) HOMO−15→LUMO+6	π→π*	

			(17%) HOMO−11→LUMO+6	π→π*
			(10%) HOMO−11→LUMO+8	π→π*
			(20%) HOMO−11→LUMO+11	π→π*
			(12%) HOMO−10→LUMO+6	π→π*
			(13%) HOMO−10→LUMO+11	π→π*
			(17%) HOMO−7→LUMO+11	π→π*
			(35%) HOMO−3→LUMO+6	π→π*
			(17%) HOMO−3→LUMO+11	π→π*
T_7	3.7863	327.46	(21%) HOMO−17→LUMO+5	π→π*
			(10%) HOMO−16→LUMO+5	π→π*
			(25%) HOMO−14→LUMO+5	π→π*
			(10%) HOMO−12→LUMO+5	π→π*
			(15%) HOMO−12→LUMO+8	π→π*
			(12%) HOMO−12→LUMO+9	π→π*
			(14%)HOMO−12 →LUMO+10	π→π*
			(10%) HOMO−11→LUMO+8	π→π*
			(10%) HOMO−11→LUMO+10	π→π*
			(12%) HOMO−5→LUMO+5	π→π*
			(11%) HOMO−4→LUMO+5	π→π*
			(33%) HOMO−2→LUMO+5	π→π*
T_8	3.7951	326.70	(14%) HOMO−16→LUMO+7	π→π*
			(17%) HOMO−12→LUMO+7	π→π*
			(20%) HOMO−10→LUMO+9	π→π*
			(16%) HOMO−10→LUMO+12	π→π*
			(28%) HOMO−9→LUMO+5	π→π*
			(17%) HOMO−9→LUMO+9	π→π*
			(10%) HOMO−9→LUMO+11	π→π*
			(12%) HOMO−6→LUMO+7	π→π*
			(17%) HOMO−5→LUMO+7	π→π*
			(27%) HOMO−4→LUMO+7	π→π*
T_9	3.8104	325.39	(11%) HOMO−13→LUMO	π→π*
			(61%) HOMO−13→LUMO+1	π→π*
			(11%) HOMO−12→LUMO+1	π→π*
			(18%) HOMO−11→LUMO+1	π→π*
			(10%) HOMO−10→LUMO+1	π→π*
T_{10}	3.8766	319.82	(63%) HOMO−18→LUMO	π→π*
			(14%) HOMO−15→LUMO	π→π*
			(24%) HOMO−3→LUMO	π→π*
			(13%) HOMO→LUMO	π→π*

Table S5 The CIE chromaticity diagram of **EuL** and **EuL**@PMMA excited at different wavelength.

EuL			**EuL**@PMMA		
λ_{ex}	X	Y	λ_{ex}	X	Y
255	0.37	0.34	255	0.29	0.30
265	0.40	0.34	265	0.30	0.31
275	0.41	0.34	275	0.31	0.32
285	0.45	0.34	285	0.34	0.32
295	0.50	0.34	295	0.38	0.32
305	0.53	0.34	305	0.41	0.32
315	0.47	0.33	315	0.36	0.30
325	0.47	0.33	325	0.22	0.26
335	0.32	0.32	335	0.19	0.26
345	0.26	0.32	345	0.19	0.27
355	0.23	0.31	355	0.19	0.27
365	0.23	0.30	365	0.19	0.26

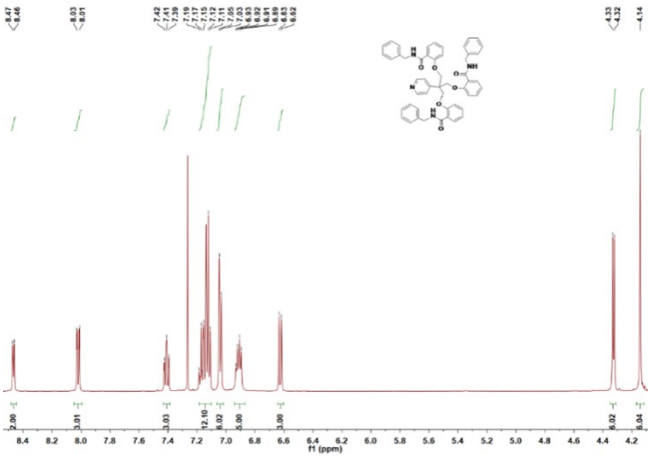

Fig. S1 ^{1}H NMR spectra of the ligand **L**.

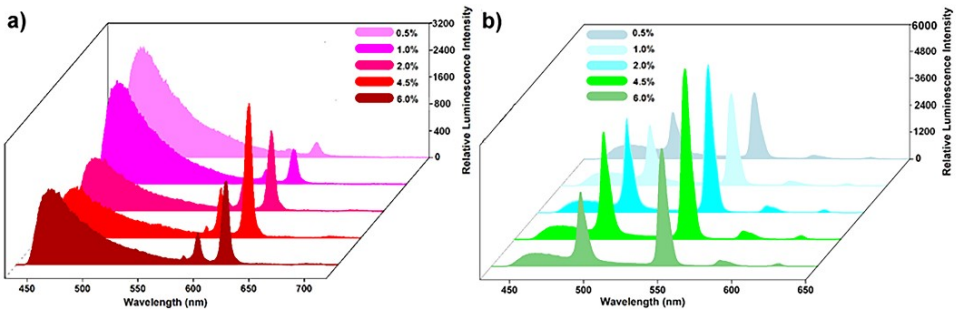

Fig. S2 The emission spectra of **EuL**@PMMA(a) and **TbL**@PMMA (b) with different doping ratios.

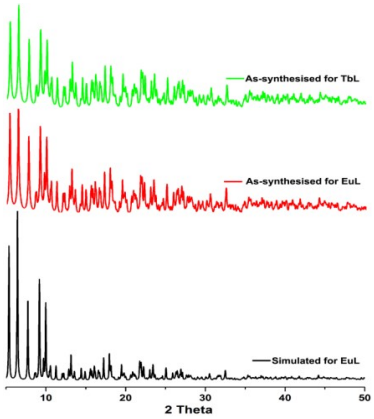

Fig. S3 The PXRD patterns of **EuL**, **TbL** and that of simulated from CIF files.

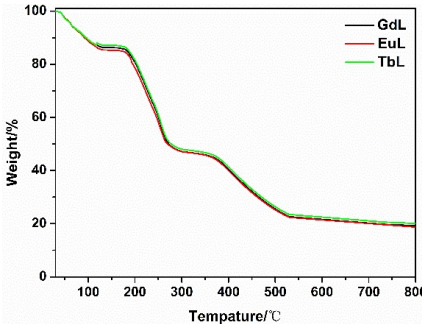

Fig. S4 TG curves of **EuL**, **TbL** and **GdL** from 30℃ to 800℃.

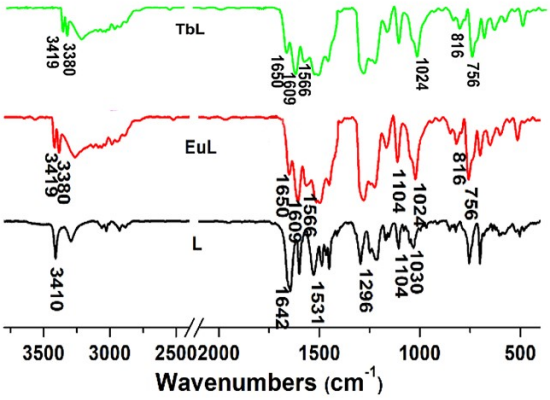

Fig. S5 The IR spectrum of **L**, **EuL** and **TbL**.

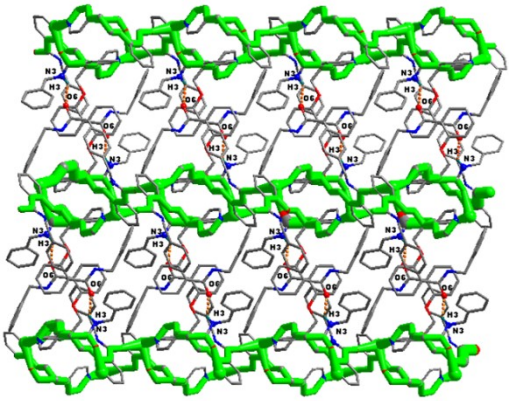

Fig. S6 The 3D supramolecular architecture of **TbL** constructed by N3–H3···O6 hydrogen bond.

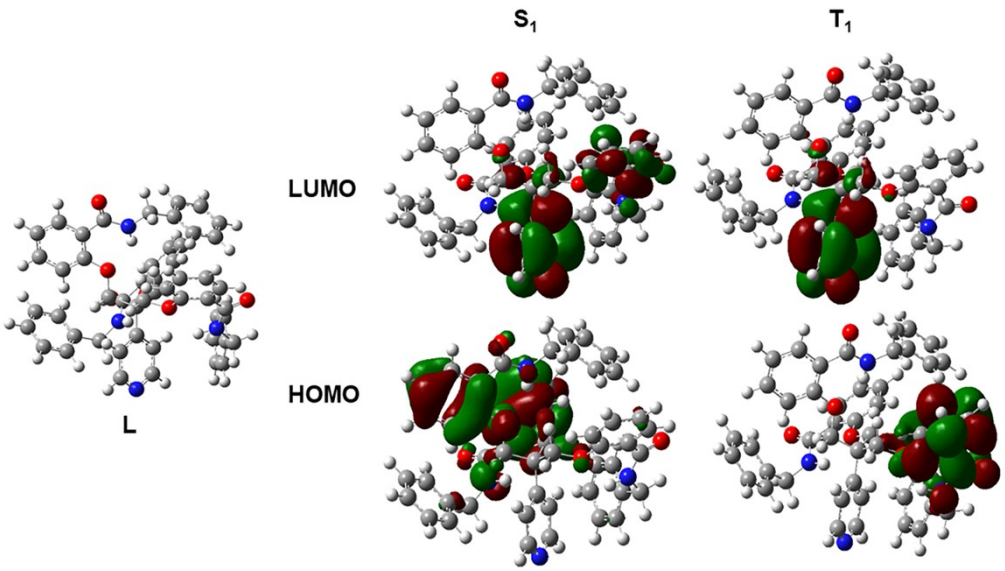

Fig. S7 The HOMO and LUMO of **L** in singlet and triplet state for **EuL** and **TbL** calculated by the DFT methods.

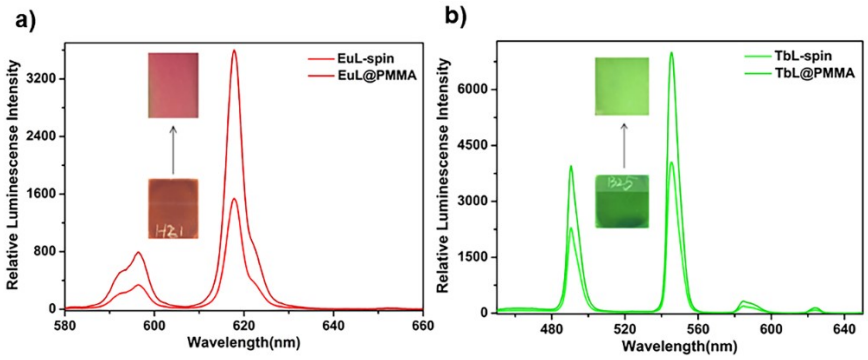

Fig. S8 The emission spectra of two kinds films for **EuL**(a), **TbL**(b)with doping ratio of 4.5% excited at 315 nm.

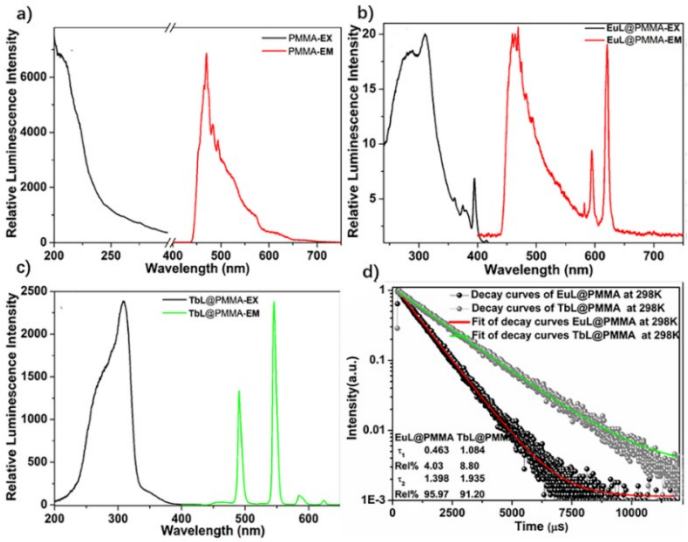

Fig. S9 The excitation and emission spectra of PMMA (a), **EuL**@PMMA (b) and **TbL**@PMMA (c) excited at 315 nm; The decay curve of $^5D_0$ in **EuL**@PMMA and that of $^5D_4$ state in **TbL**@PMMA (d).

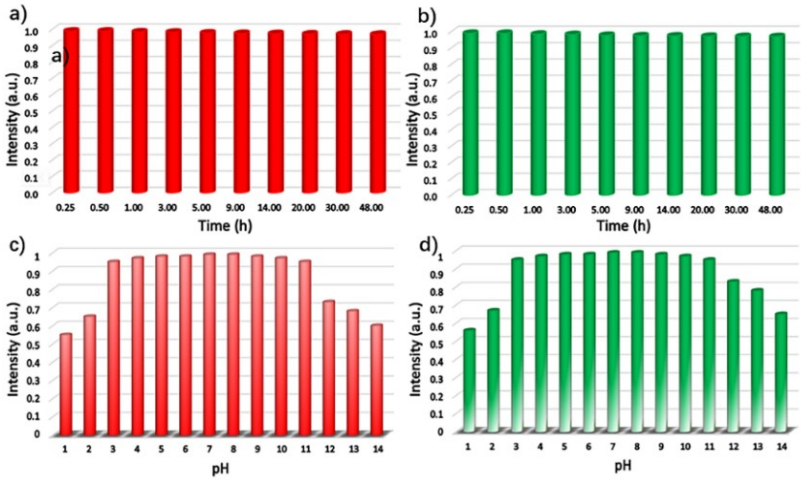

Fig. S10 The luminescence intensity of **EuL**/**TbL**@PMMA that immersed in water for different time(a), (b) and different pH (c), (d).

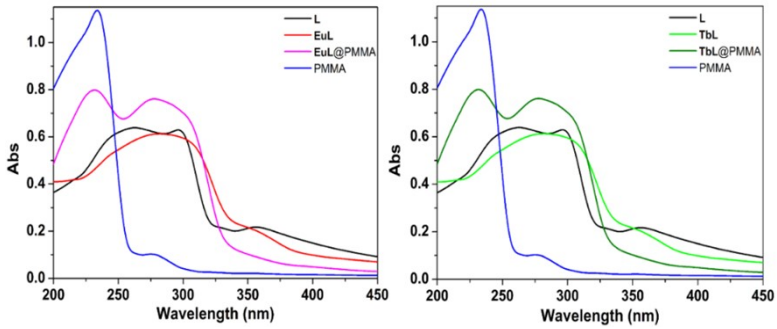

Fig. S11 The UV-Vis absorption spectrum of **L**, **EuL**/**TbL**, **EuL**/**TbL**@PMMA and PMMA.

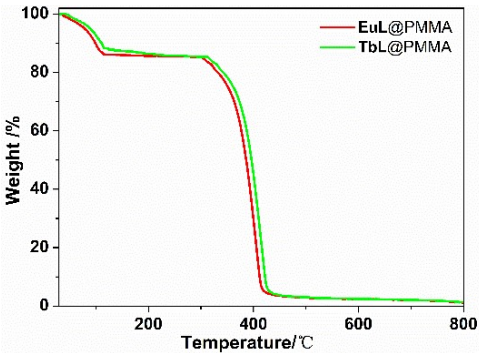

Fig. S12 TG curves of **EuL**@PMMA and **TbL**@PMMA from 30℃ to 800℃.

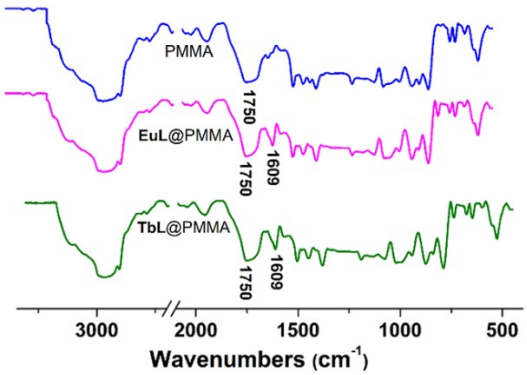

Fig. S13 The IR spectrum of PMMA，**EuL**@PMMA and **TbL**@PMMA.

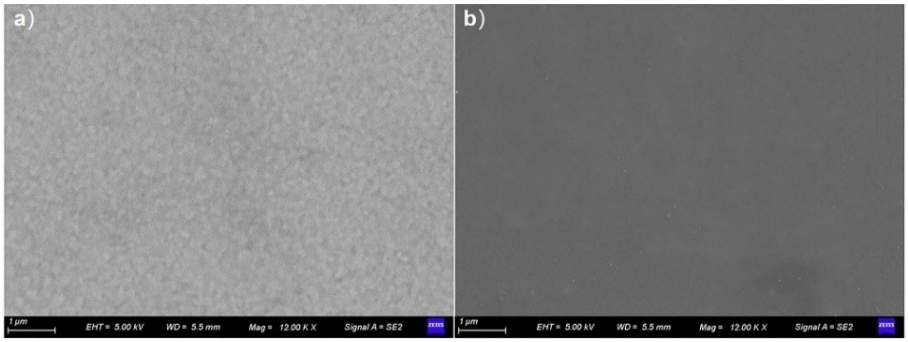

Fig. S14 SEM image of spin-coated film (a) and that doped with PMMA(b).

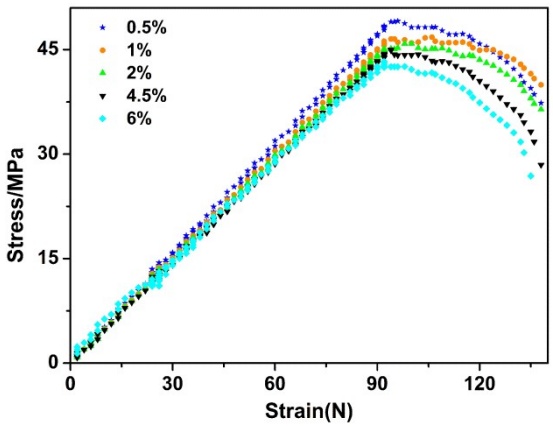

Fig. S15 Typical stress−strain curves of **EuL**/**TbL**@PMMA with different mass percentage.

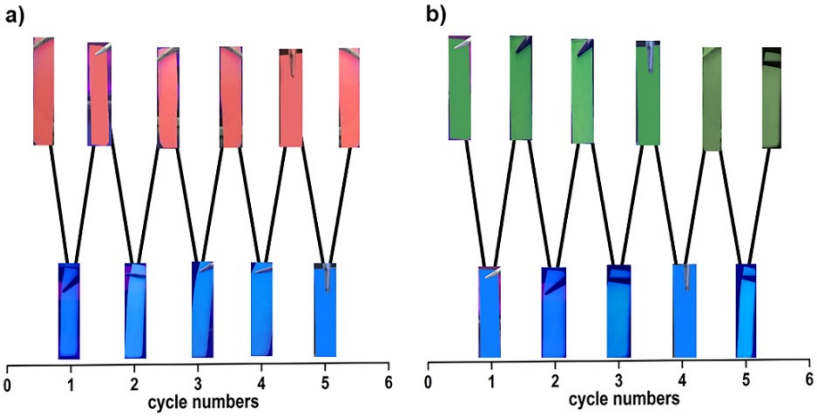

Fig. S16 The sensing and recovery tests of **EuL**@PMMA(a) and **TbL**@PMMA(b) for NH_3.

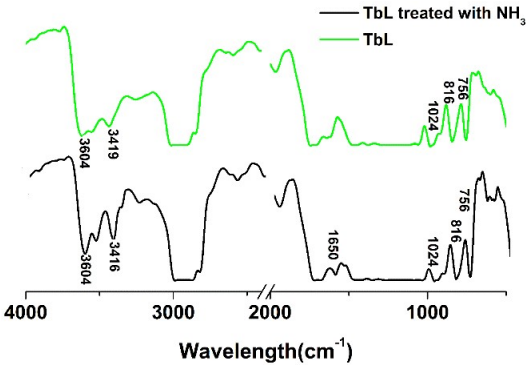

Fig. S17 Infrared spectroscopy of **TbL**@PMMA before and after the reaction with ammonia.

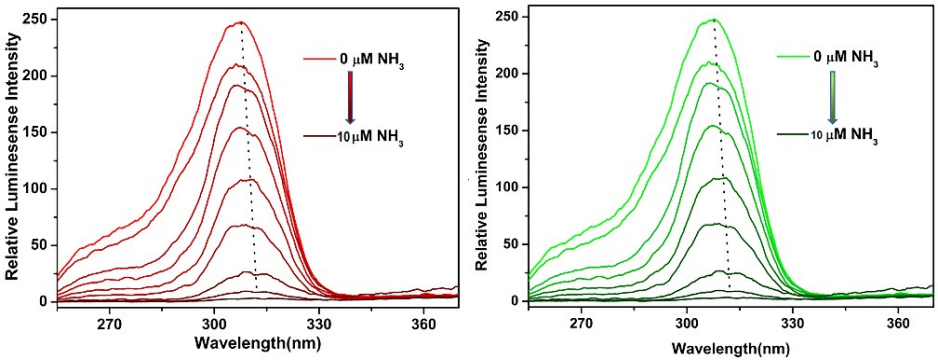

Fig. S18 The excitation spectrum of **EuL**/**TbL**@PMMA that immersed in ammonia at different concentration.

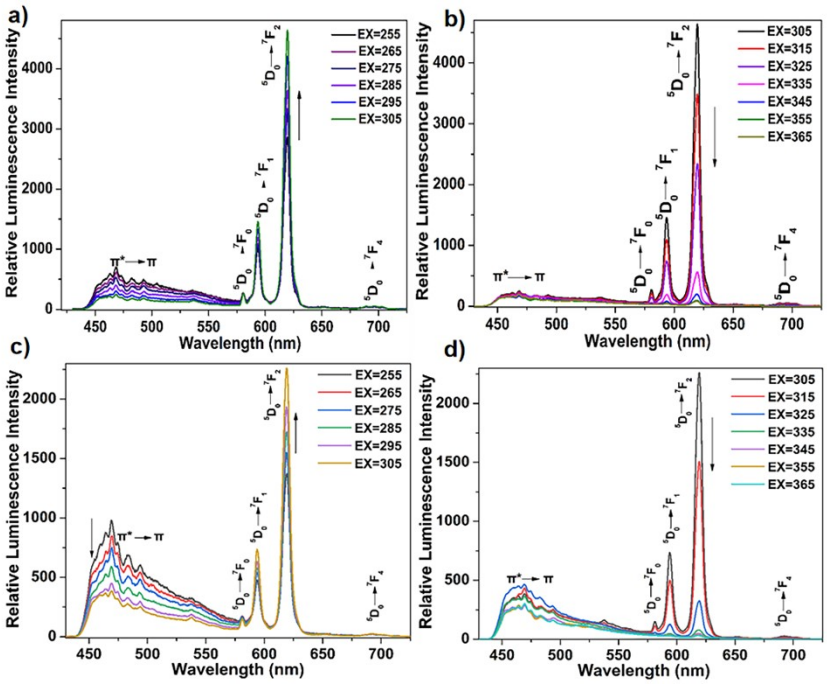

Fig. S19 Upon excited from 255nm to 365 nm with a 10 nm grades, the emission spectrums of **EuL**(a) and (b), **EuL**@PMMA(c) and (d).

Reference

1 G. M. Sheldrick, SHELXTL, Reference Manual: version 5.1: Bruker AXS, Madison, WI, **2014**.

2 DIAMOND. version 3.1; Crystal Impact: Bonn, Germany, **2004**.

3 X. Q. Song, H. H. Meng, Z. G. Lin and L. Wang, 2D Lanthanide Coordination Polymers: Synthesis, Structure, Luminescent Properties, and Ratiometric Sensing Application in the Hydrostable PMMA-Doped Hybrid Films, *ACS Appl. Polym. Mater.*, **2020**, 4, 1644−1655.